MEASUREMENTS OF FLOW PATTERNS AND VELOCITIES OF GAS-WATER TWO-PHASE FLOWS USING ELECTRICAL RESISTANCE IMAGING

Y. Wu*, M. Wang+, H. Li*, D. Li*, R. A. Williams+, Z. Zheng*
***Institute of Mechanics, Chinese Academy of Sciences, Beijing, 100080, P.R. China, yxwu@imech.ac.cn**
+Institute of Particle Science and Engineering, University of Leeds, Leeds, LS2 9JT, UK, m.wang@leeds.ac.uk

ABSTRACT
This paper presents a measurement of flow patterns and flow velocities of gas-water two-phase flows based on the technique of electrical resistance tomography (ERT) in a 40m horizontal flow loop. A single-plane and dual-plane ERT sensor on conductive ring technique were used to gather sufficient information for the implementation of flow characteristics particularly flow pattern recognition and air cavity velocity measurement. A fast data collection strategy was applied to the dual-plane ERT sensor and an iterative algorithm was used for image reconstruction. Results, in respect to flow patterns and velocity maps, are reported.
Keywords: ERT, gas-water two-phase flow, velocity measurement, flow pattern.

1. INTRODUCTION
In petroleum industry, multiphase flow of gas and liquids is commonly encountered in the production and transportation of oil and gas, such as the oil that flows to the surface is often accompanied by gas and pipeline flow may also contain two or more flowing phases. Therefore, the need for multiphase flow measurement in the oil and gas production has been evident for many years. Multiphase flow measurement has yet to be established as a separate discipline.
The complexity in multiphase flow measurement lies in the simultaneous existence of the gas and liquid phases. The interface between the phases (gas-liquid and liquid-liquid) can be distributed in many configurations which are called flow patterns, demonstrate a very important feature of gas-liquid multiphase flows. In single-phase flow in pipes, the design parameters such as pressure drop can be calculated in a relatively straightforward way, while the existence of other phases presents can difficult challenge in understanding and modelling the flow system. The hydrodynamics of the flow, as well as the flow mechanisms, change significantly from one flow pattern to another. For instance, it has been demonstrated that for similar flow conditions, slug flow and wavy flow may result in a difference in pressure drop of a factor of two.
In petroleum multiphase transportation engineering, the most important parameters which engineers want to know are the pressure drop and the flowrate of each phase.
The pressure drop of a two-phase flow is described by:

$$-\Delta p_{TP} = -\Delta p_f - \Delta p_a - \Delta p_g \tag{1}$$

where $(-\Delta p_{TP})$ is the pressure drop of a two-phase flow, $(-\Delta p_f)$ is the pressure drop resulted from friction of the flow, $(-\Delta p_a)$ is the pressure drop due to the acceleration of the flow, and $(-\Delta p_g)$ attribute to the hydrostatic pressure. The equation of the pressure drop of a two-phase flow can be written as expanded form of that for single phase flow. The difficulty in this manner is that local values of important variables such as in-situ velocities and holdups of the individual phases are not known and cannot readily be predicted. If there are more than two phases, the situation will be much more complex. Anyway, it is obviously that the information of local velocity, the hold-ups of individual phases and the flow pattern recognition is needed.
In order to measure the mass flow rate (M) of oil, gas and water components in the flow, an inferential mass method can be used which requires both the instantaneous velocity and cross-sectional fraction of each phase in order to calculate the individual component mass flowrates and total mixture mass flowrate M. Therefore, it is necessary to measure the distribution of the local volume fraction (α_i), and the distribution of the local axial velocity (V_i). The mass flowrate M can then be taken as:

$$M = \int_A \rho_i \alpha_i V_i dA \quad \text{or} \quad M/A = \alpha_G \rho_G V_G + \alpha_W \rho_W V_W + \alpha_O \rho_O V_O \tag{2}$$

where A is the cross section.
Since density information on the oil, water and gas phases is readily available from other parts of the production process, the problem is therefore to measure the oil, water and gas velocity (V_O, V_G and V_W) and two of the phase fractions (usually gas void fraction α_G and water fraction α_W).

Process tomography is a discipline which has been a significant growth over the last ten years, and is becoming increasingly promising in the study and application of multiphase flows. This is due to its non-intrusive nature and potential capacity for providing a means of 'looking' inside the detailed local flow information such as volume fraction, the velocity distribution of individual phases and the inter-phase behaviour [1].

In this paper, electrical resistance tomography (ERT) technique is adopted to study the flow pattern and the velocity distribution in a gas-water two-phase horizontal flow [2-3]. The flow pattern was obtained by stacking the images according to the time sequence after the image has been reconstructed which gives a good means of recognising flow regime structure. Of course, the flow pattern analyse by computer does require advanced pattern recognition techniques, which is under development. In order to use cross correlation technique to perform component velocity measurement, a dual-plane ERT sensor on conductive ring technique was used to gather sufficient information for the implementation of the velocity of the dispersed phase. A fast data collection strategy was applied to the dual-plane ERT sensor and an iterative algorithm was used for image reconstruction [4], and much improved velocity profiles of the gas phase in an air/water flow at different flow patterns were reported.

2. EXPERIMENTAL SET-UP

All the experiments described in this paper were carried out using the multiphase flow loop made of transparent Perspex at Institute of Mechanics, Chinese Academy of Sciences, which is a 40 m horizontal gas-liquid flow loop with an inner diameter of 50mm.

The flow loop is fully made of transparent Perspex. It can run a maximum superficial liquid velocity of 1.2 m/s with Reynolds number about 40,000, and a superficial gas velocity of 30 m/s with Reynolds number about 100,000. The two-phases of gas and liquid, in terms of flow states of laminar to laminar, laminar to turbulent, turbulent to laminar and turbulent to turbulent, can be performed on this test-loop. By controlling the pressure and flowrates of the gas phase and the liquid phase, many flow patterns, such as bubbly flow, stratified flow, plug flow, slug flow, wavy flow and annular flow, can be created in this device. The pressure, pressure difference and velocity of two-phase components are monitored using a number of pressure sensors and hot-film sensors. A tomographic sensor with three sensing planes is also installed in the flow loop in order to obtain flow patterns of particulate two-phase flow.

The tap-water (conductivity 0.304mS/cm) was used as the liquid phase, and air was introduced into the flow loop from a mixing jet-pump as the gas phase. Measurements were performed at ambient temperature. By controlling the air flowrate at the air inlet of the jet-pump, different flow patterns can be generated in the flow loop.

The experiments were performed under different air flowrates of $0.5m^3/h$, $1.5m^3/h$, $4m^3/h$, $10m^3/h$ and some less than $0.5m^3/h$ in regard to the productions of bubbly flow, slug flow, slug-churn flow, and churn flow regimes. The water flows were scaled with an accumulating tank during the experiments to get water flowrate and mean velocity. At the mean time, a number of photographs were recorded as visual presentations of these different flow patterns.

3. THE ERT SYSTEM

3.1 ERT Hardware System

A P2000 ERT system (Industrial Tomography System Ltd., Manchester) was used for data collection. The so-called adjacent electrode pair strategy [5] was adopted, using a 15mA injection current at 9.6 kHz. Data collection rates were 50ms per frame at the signal frequency of 9.6 kHz and 16 ms per frame at the signal frequency of 38.4 kHz. Both single-plane and dual-plane ERT sensors were used in this study. Each ERT sensing plane consists of 16 titanium-alloy rectangular electrodes (5mm×12mm).

3.2 ERT Sensor Set-up

A single-plane and dual-plane ERT sensor on conductive ring technique were used in this study. The dual-plane ERT sensor is a core sensing technique in the experiment for implementation of local flow velocities in the two-phase flow. Since the current data collection speed was still limited, we set the distance between the two sensing planes apart further to 590mm. To improve the correlation, a dual-plane measurement strategy was applied, which was built in the ITS P2000 ERT system. The principle of the dual-plane strategy is based on a 'cross measurement between two correlated electrodes on two sensing planes' instead of 'plane by plane' measurement. SBP (sensitivity coefficient weighted back-projection) algorithm was used for on-line flow pattern recognition due to its fast image reconstruction speed. An off-line multi-step algorithm, known as SCG algorithm (the sensitivity theorem based inverse solution using generalized conjugate gradients methods with a method of error vector decomposition) [4], was utilized for the image reconstruction in the velocity implementation in order to reduce the error caused by the point-spread function in the use of the SBP algorithm. The SCG algorithm employs a multi-step approach with the sensitivity theorem based linear approximation and the differences between the relative changes in the measured and simulated boundary voltages at each step to solve the non-linear electric field inverse problem. All images used for implementation of local velocities in the paper were reconstructed with the SCG algorithm.

The dimension of the sensing planes installation is given in Figure 1, and a photograph of the set-up is shown in Figure2.

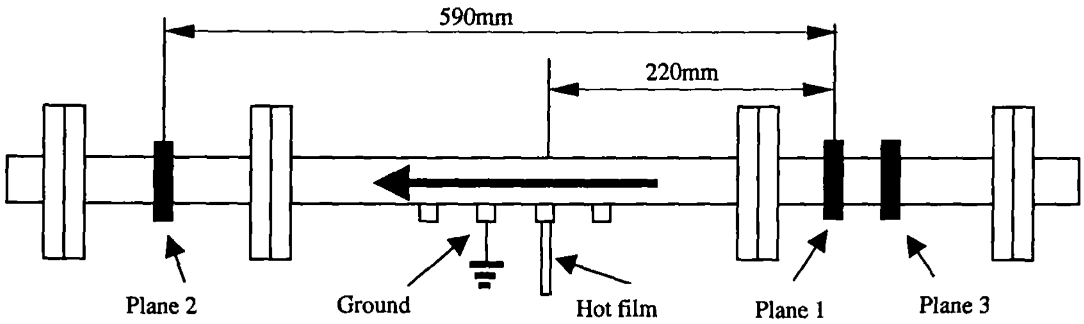

Fig. 1 Sensor configuration

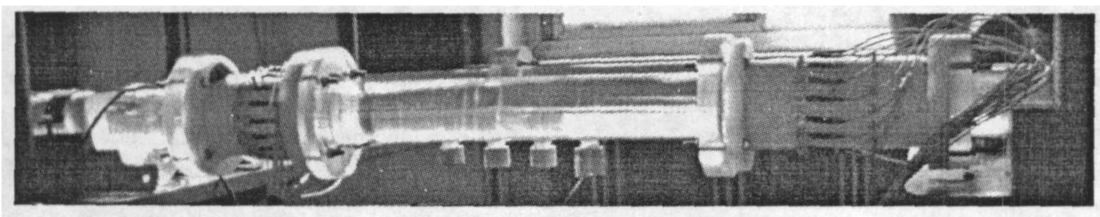

Fig. 2 The photograph of the sensor

3.3 Flow Parameter Calculation Using ERT

The local axial velocity can be obtained by applying the cross-correlation technique to determine the speed of moving profiles [6-7]. The basic function of the cross-correlation technique is to find the time offset between two signals where the similarities are most obvious. These signals can be any value and are not limited to quantitative conductivity data. This goal is to find a transition time τ that corresponds to the minimum difference (ε) . This can be achieved by using the least square criterion as the following equation:

$$\varepsilon^2_{xy}(\tau) = \min \lim_{T\to\infty} \frac{1}{T} \int_{-T}^{T} [x(t) - y(t-\tau)]^2 \, dt \tag{3}$$

where x, y are the original signals of void fraction at each imaging cross section respectively, ε is the error function which gives the transition time τ when the expression take a minimum value.

Replacing the integral by partial summation, equation (3) can be expressed in discrete form:

$$\varepsilon_k^2(n) = \sum_{m=0}^{N} [x_k(m) - y_k(m-n)]^2 \tag{4}$$

where N is the sample length, n is the sample offset number and k is the number to indicate different pixels on the cross-section.

In the computation, N should be selected according to the distance between the dual-plane ERT sensors and the maximum and the minimum velocity of the flow. N is selected amongst 100~700 (images) in this study.

It should be noted that equation (3) could be deduced to the following form:

$$\begin{aligned} \varepsilon^2_{xy}(\tau) &= \min \lim_{T\to\infty} \frac{1}{T} \int_{-T}^{T} [x(t) - y(t-\tau)]^2 \, dt \\ &= \min \lim_{T\to\infty} \frac{1}{T} \int_{-T}^{T} \left[x(t)^2 + y(t-\tau)^2 - 2x(t)y(t-\tau) \right] dt \end{aligned} \tag{5}$$

The equivalent form of the above equation is:

$$R = \max \lim_{T\to\infty} \int_{-T}^{T} x(t) \cdot y(t-\tau) dt \tag{6}$$

or, in a discrete form of a partial summation:

$$R_k(n) = \sum_{m=0}^{N} x_k(m) \cdot y_k(m-n) \tag{7}$$

Equation (6) and (7) were recognised as short forms of equation (3) and (4) and have been utilised in some cross correlation calculation. However, we found that in obtaining the velocity profiles of a multiphase flow from ERT imaging data, equation (3) or (4) should be used to avoid larger errors because of only a finite integral range being applied other than an infinite integral range in equation (3). Furthermore, it is not always true that in a practical correlation, the integral of $y(t-\tau)^2$ over the range maintains unchanged. We thus propose directly applying equation (3) or its discrete form (4) to carry out cross-correlation when needed as we did in the study.

4. EXPERIMENT RESULTS

4.1 Flow Pattern Recognition

Flow pattern recognition was obtained with data from the single-plane ERT sensor (plane 3 in Figure 1). The data collection speed used in this mode was 62 frames/sec, and images were reconstructed by using SBP algorithm. By stacking part of reconstructed tomograms, gas-phase and liquid-phase distribution and their dynamical varying processes (flow processes) in the pipe can be clearly demonstrated. Flow patterns varied with air flowrates are illustrated in Figure 3 resulted from ERT reconstruction.

Bubbly flow (superficial water velocity: 0.609m/s, superficial air velocity: 0.004 m/s)

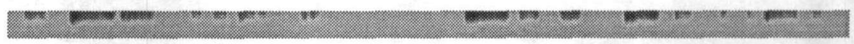

Bubbly flow (superficial water velocity: 0.605m/s, superficial air velocity: 0.007 m/s)

Bubbly flow (superficial water velocity: 0.605m/s, superficial air velocity: 0.014 m/s)

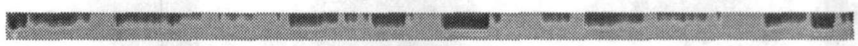

Short slug flow (superficial water velocity: 0.590m/s, superficial air velocity: 0.035 m/s)

Long slug flow (superficial water velocity: 0.538m/s, superficial air velocity: 0.071 m/s)

Churn flow (superficial water velocity: 0.563m/s, superficial air velocity: 0.212 m/s)

Churn flow (superficial water velocity: 0.515m/s, superficial air velocity: 0.566 m/s)

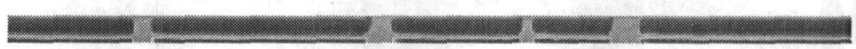

Churn flow (superficial water velocity: 0.484m/s, superficial air velocity: 1.415 m/s)

Fig. 3 Flow patterns vs. different air flowrates (black denotes air phase and grey denotes water phase)

4.2 Flow Velocity Measurement

To demonstrate the use of cross correlation in obtaining the velocity profile of a multiphase flow, some stacked images from three air flowrates (0.025 m^3/h, 0.5 m^3/h and 4 m^3/h) are given in Figure 4. The correlation between two images taken from different positions is obviously. It demonstrates the dual-plane mode at 31.3 dual-frames/second is able to manage the velocities at the demonstrated mean air flowrates.

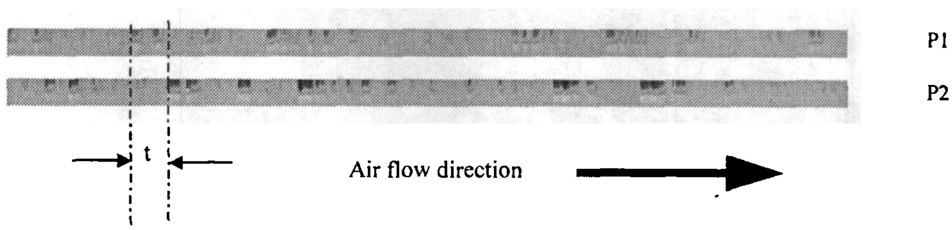

(a) Bubbly flow (superficial water velocity: 0.628m/s, superficial air velocity: 0.004 m/s)

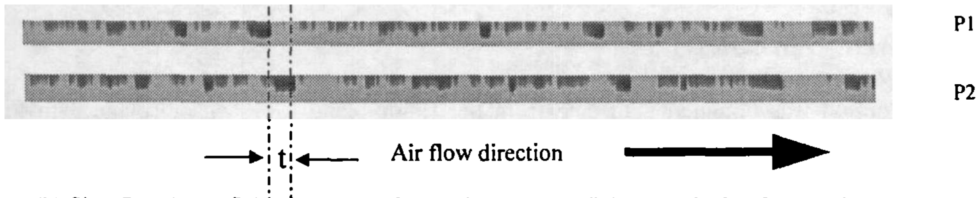

(b) Slug flow (superficial water velocity: 0.590m/s, superficial air velocity: 0.071 m/s)

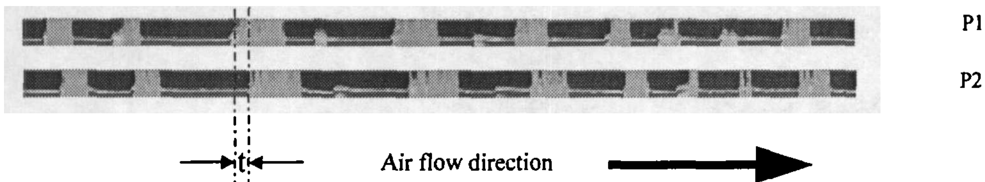

(c) Churn flow (superficial water velocity: 0.528m/s, superficial air velocity: 0.566 m/s)

Fig. 4 Cross-correlation between two images obtained from dual-plane ERT sensor

The gas-phase velocity converted from the cross-correlation results can be calculated by:

$$v = \frac{\Delta s}{\Delta t} = \frac{L}{(n_k - 1)/F_s} \tag{8}$$

where L is the distance between two sensor planes, n_k is the number of n when it makes equation (3) or (4) take the minimum value, F_s is the sampling frequency.

By applying the cross-correlation procedure to a data set of 1000-frame of tomographic images, which were acquired from the air/water two-phase horizontal pipe flow, an evident correlation was found for the similar flow information at some corresponding pixels of the dual-sensing rings. Figure 5 shows the velocity distribution, resulted from the cross-correlation implementation, for a bubbly flow, a slug flow and a churn flow. The average velocities of the gas phase implemented from the cross correlation are approximated as about 0.629 m/s, 1.009 m/s and 1.427 m/s. The superficial velocities estimated in the experiments are 0.628 m/s, 0.590 m/s and 0.528 m/s for water and 0.004 m/s, 0.071 m/s and 0.566 m/s for air at those flow patterns respectively.

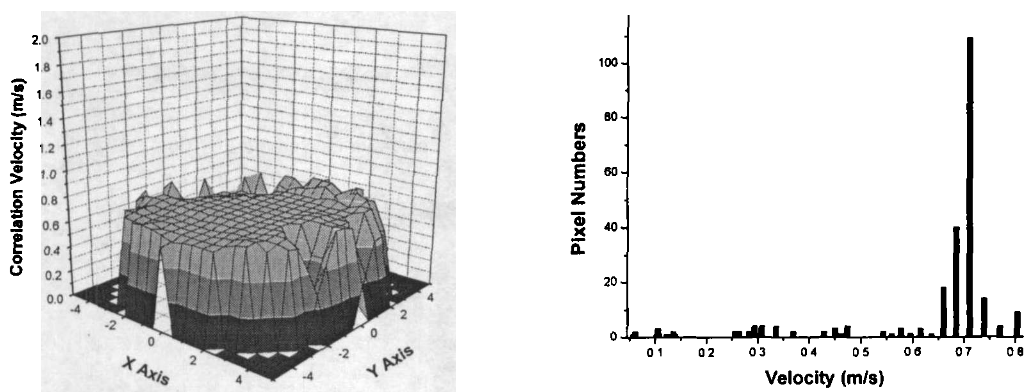

(a) Bubbly flow (superficial water velocity: 0.628m/s, superficial air velocity: 0.004 m/s)

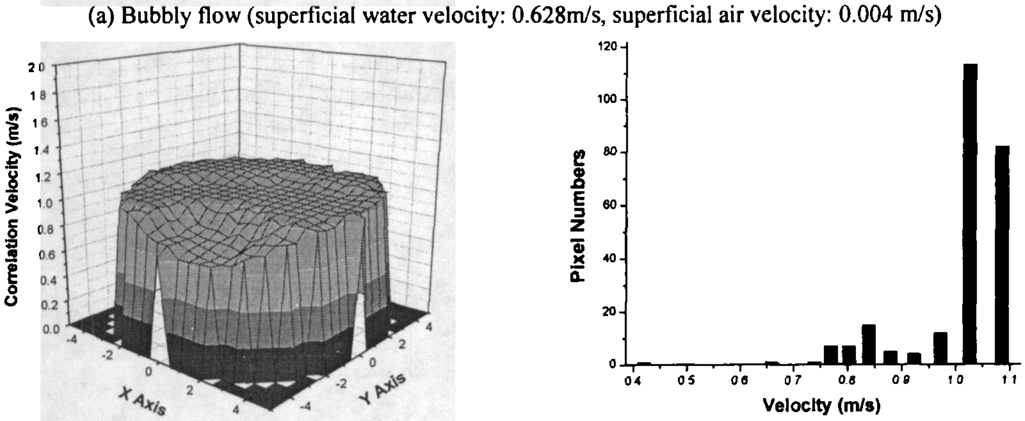

(b) Slug flow (superficial water velocity: 0.590m/s, superficial air velocity: 0.071 m/s)

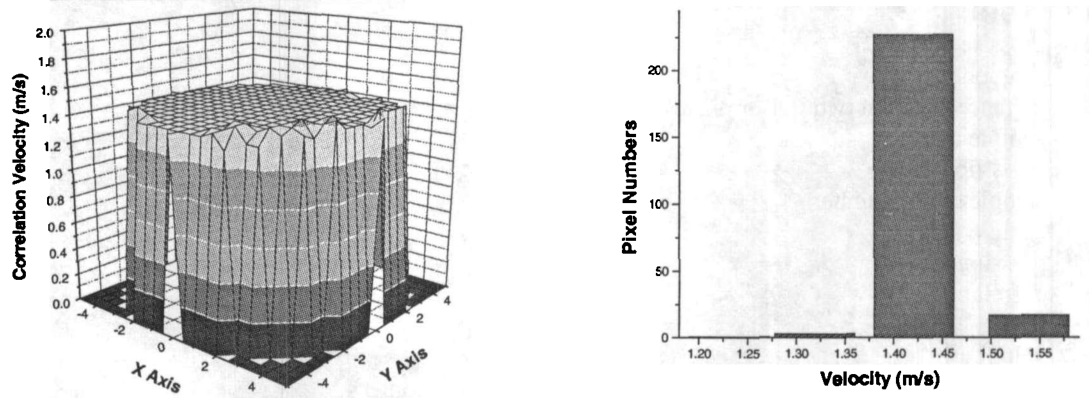

(c) Churn flow (superficial water velocity: 0.528m/s, superficial air velocity: 0.566 m/s)

Fig. 5 Correlation phase velocity distributions at different flow patterns

5. DISCUSSIONS AND CONCLUSIONS

From the main results of Figures 3, 4 and 5, some useful information and interesting phenomena can be found for both gas-liquid two-phase flow and ERT technique, viz.:

First, the ERT technique is a suitable means for detecting the flow patterns of gas-liquid multiphase flow. With a fast data collecting protocol and an effective iterative image reconstruction algorithm, gas-phase and liquid-phase distribution and their dynamic variations in the pipe can be clearly quantified (Figure 3).

Secondly, the time of cross-correlation can reveal the velocity magnitude of the interface of the gas-phase and liquid-phase. The cross-correlation time interval of bubbly flow is longer than that of slug flow, and much longer than that of churn flow (Figure 4). Based on the time interval (ERT data frames), the mean velocity of gas-liquid two-phase can be estimated. This may be important in the on-situ monitor of industrial processes.

Thirdly, the degree of the cross-correlation of the flow state increases with the increase of gas flowrate(Figure 4). This can also be proven during the cross-correlation procedure. In slug or churn flow, the cross-correlation graphics can be obtained on more pixels than that in bubbly flow.

Fourthly, it is amazing that we can almost obtain the phase distribution on the cross-section from the velocity distribution (Figure 5). In slug flow, an obvious large gas bubble locates on the top of the pipe. Based on the values of velocities (the lower part of velocity is gas-phase, and higher part is the liquid-phase), we can estimate the average velocities and phase distribution of both-phases. Why we can obtain the information of liquid-phase so obviously and correctly by cross-correlation? We think it is due to the velocity of gas-phase is lower than the velocity of liquid-phase for the effect of friction, maybe some fine gas bubbles mixed in the liquid and their velocities are approximately the same as the liquid, and ERT can detect their information (conductivity) and gives the feature of liquid-phase during the cross-correlation.

Lastly, based on the data of velocity distribution and phase distribution from ERT reconstruction data and cross-correlation data, it is promising to obtain the flowrates of both phases. The further work is left as the future efforts.

ACKNOWLEDGEMENTS

The authors gratefully acknowledge the supports of Royal Society-Chinese Academy of Sciences (under Joint Project: Q783), CAS & CNOOC (under grant KJCX2-SW-L03), and National 863 Project (under the project number 2001AA413210).

REFERENCES

1. M.Wang and W.Yin, Measurements of the Concentration and Velocity Distribution in Miscible Liquid Mixing Using Electrical Resistance Tomography, Tras IChemе, 79, Part A, pp. 883-886, 2001.
2. M.Wang, A.Dorward, D.Vlaev and R.Mann, Measurement of Gas-Liquid Mixing in a Stirred Vessel Using Electrical Resistance Tomography(ERT), Chem. Eng. J. 77, pp. 93-98, 2000.
3. R.Mann, M.Wang, A.E.Forrest, P.J.Holden, F.J.Dickin, T.Dyakowski and R.B.Edwards, Gas-Liquid and Miscible Liquid Mixing in a Plant-Scale Vessel Monitored Using Electrical Resistance Tomography, Chem. Eng. Comm, 175, pp. 39-48, 1999.
4. M.Wang, Inverse Solutions for Electrical Impedance Tomography Based on Conjugate Gradients Methods, Measurement Science and Technology, 13, pp. 101-117, 2002.
5. B.H.Brown and A.D.Segar, Applied potential tomography: Data collection problems, Proc IEE Int Conf on Electric and Magnetic Field in Medic and Biolo, pp 79-82, 1985.
6. M.S.Beck and A.Plaskoeski, Adam Hilger, Bristol, UK, 1987.
7. G.P.Lucas, I.Cory, R.Waterfall, W.W.Loh and F.J.Dickin, Journal of Flow Measurement and Instrumentation, 10(4), 1999.

NOMENCLATURE

A	cross section area
F	frequency
L	distance between two sensor planes
m	sample number
M	mass flow rate
n	sample offset number
N	sample length
p	pressure
R	correlation error
t, T	time
v, V	velocity
x, y	original signals of void fraction at each imaging cross section
α	local volume fraction
ρ	density
ε	correlation error
τ	transition time

Subscripts

a	acceleration
f	friction
g	gravity
G	gas
i	individual
k	pixel number
O	oil
s	sample
TP	two-phase flow
W	water
x, y	original signals of void fraction at each imaging cross section